

Symbolic dynamics approach to find periodic windows: the case study of the Rössler system

Zbigniew Galias*

Abstract

Modification of a parameter of a chaotic system may lead to the emergence of a periodic attractor. Under certain assumptions periodic windows (regions in the parameter space in which a periodic attractor exists) densely fill a chaotic region. Usually it is very difficult to prove this property. In this work, we propose a systematic procedure to locate and prove the existence of periodic windows. The method combines the symbolic dynamics based approach to find unstable periodic orbits (UPOs), the continuation method to locate periodic windows (PWs), and interval arithmetic tools to prove their existence. The proposed method is applied to the Rössler system. The existence of several thousands of PWs close to the classical parameter values is proved and periodic attractors very close in the parameter space to the classical Rössler attractor are found. Estimates of measures of sets of parameters for which a periodic attractor exists are calculated.

Keywords: periodic window, Rössler system, symbolic dynamics, continuation method, rigorous numerical analysis, computer-assisted proof.

1 Introduction

Dynamical systems which exhibit a transition to chaos via a cascade of period-doubling bifurcations often support a sequence of periodic windows which densely fill the chaotic region [1–3]. Periodic windows may be observed in bifurcation diagrams of such systems. Narrow periodic windows are virtually impossible to see when sampling the parameter space due to requirements of very fine sampling and long convergence times [4, 5].

In this study an efficient method to find and prove the existence of periodic windows (PWs) is presented. We use a combination of the symbolic dynamics based method to find unstable periodic orbits (UPOs) embedded in numerically observed chaotic attractors for selected points in the parameter space, the continuation method to locate PWs in the region of interest and interval arithmetic tools to prove the existence of periodic attractors. The method is applied to analyze the existence of periodic windows for the Rössler system [6] close to the classical case $(a, b) = (5.7, 0.2)$. We aim at finding a large number of periodic windows providing a good approximation of the measure of the set of regular parameter values for which periodic attractors exist. We also want to find periodic attractors as close to the classical case as possible.

Investigations of the existence of periodic orbits (cycles) and periodic windows for the Rössler system [6] are carried out by many researchers. Symbolic dynamics representation of cycles for the Rössler system is studied in [7]. The authors extract all periodic orbits with periods $p \leq 11$ of the associated return map and develop some rules of growth and pruning of the populations of periodic orbits. The existence of topological chaos for the Rössler system using the method of covering relations and the existence of infinitely many cycles is proved in [8]. A rigorous method based on the interval Newton operator and generalized bisection technique to find all short periodic orbits is developed in [9]. The method is used to locate all periodic orbits with periods $p \leq 20$. Rigorous numerical methods are used in [10] to validate a part of the bifurcation diagram. The authors prove the existence of two period-doubling bifurcations and the existence of a branch of periodic points connecting them. Various types of attractors existing for the Rössler model are studied in [11]. Using non-rigorous computations, the authors search for periodic and chaotic regions in the parameter space using various chaos indicators such as the maximum Lyapunov exponent (MLE) or the OLIF2 chaos indicator. Statistical properties of UPOs embedded in the Rössler attractor are investigated in [12]. Homoclinic chaos in the Rössler system is studied in [13]. Using symbolic approach the authors study homoclinic bifurcations and detect regions of structurally stable and chaotic dynamics in the parameter space of the Rössler model. A connection between chaotic and

*Z. Galias is with the AGH University of Krakow, Department of Electrical Engineering, 30-059 Krakow, Poland (e-mail: galias@agh.edu.pl).

hyperchaotic trajectories in a four-dimensional Rössler system is proved in [14]. Conditions for the existence of a Hopf bifurcation in the Rössler system are formulated in [15]. An extension of the Sharkovskii theorem for the Rössler system is proposed in [16].

In the remaining part of this paper we define the Rössler system in Section 2. In Section 3 a procedure to find periodic windows is presented. Symbolic dynamics representations of trajectories is introduced and methods to reduce the number of symbol sequences needed to find UPOs for a fixed parameter value and PWs in a given region of the parameter space are described. A method to prove the existence of periodic attractors is recalled. Properties of periodic windows associated with primary and period-tupling periodic symbol sequences are discussed. A study of the existence of PWs for the Rössler system in a region of the parameter space close to the classical case $(a, b) = (5.7, 0.2)$ is carried out in Section 4. Two cases are considered. First, the parameter $b = 0.2$ is fixed and $a \in [5.6, 5.8]$ is treated as a bifurcation parameter. In the second case $a = 5.7$ and $b \in [0.175, 0.215]$ is treated as a bifurcation parameter. For each case periodic orbits existing for endpoints of the considered parameter range are found. Next, periodic orbits found for the endpoints are continued to locate PWs in the region of interest. The existence of periodic windows is proved using the interval Newton method. Their widths are estimated using the continuation method and the (non-rigorous) Newton method.

For the interval computations the CAPD library [17, 18] is used. For the multiprecision computations the GNU MPFR library [19] is used.

2 The Rössler system

The Rössler system [6] is three-dimensional continuous time dynamical system defined by:

$$\begin{aligned}\dot{x} &= -y - z, \\ \dot{y} &= x + cy, \\ \dot{z} &= b + z(x - a).\end{aligned}\tag{1}$$

We consider the case where the parameters b and c are equal. Under this assumptions the Rössler system is a two-parameter family of three-dimensional vector fields. An example trajectory of the Rössler system observed for the classical case $(a, b) = (5.7, 0.2)$ is shown in Fig. 1(a).

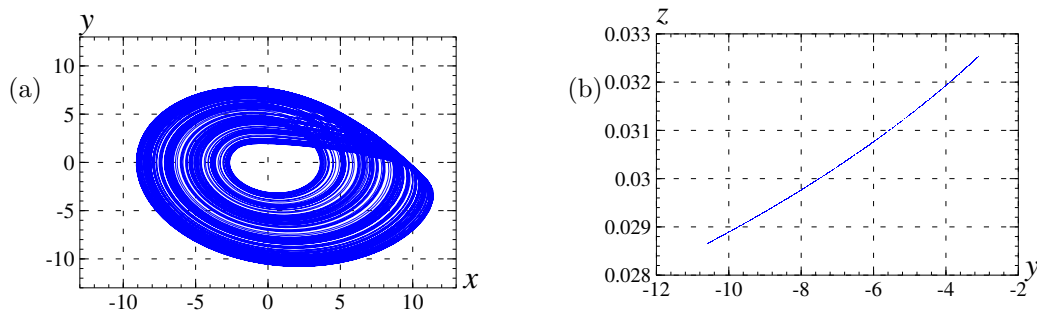


Figure 1: Example trajectories of the Rössler system for $a = 5.7$, $b = 0.2$; (a) a trajectory of the flow, (b) a trajectory of the return map $P_{a,b}$.

Let us fix the parameters a, b . To define the *return map* $P_{a,b}$ we select the return plane $\Sigma = \{v = (x, y, z) \in \mathbb{R}^3 : x = 0, \dot{x} = -y - z > 0\}$. Let us denote by $\varphi(t, v)$ the trajectory of the system (1) started at v . We will use the local coordinate system $u = (y, z)$ for points in Σ . For $v = (0, y, z) \in \Sigma$ let us denote by $\tau(v)$ the smallest positive t for which the trajectory started at v returns to Σ , i.e. $\varphi(t, v) \in \Sigma$. The image of $u = (y, z)$ under $P_{a,b}$ is defined as $(0, P_{a,b}(u)) = \varphi(\tau(v), v)$. A trajectory of $P_{5.7, 0.2}$ is plotted in Fig. 1(b).

3 Finding Periodic Windows

Construction of bifurcation diagrams is a standard method to find periodic windows (PWs).

Bifurcation diagrams with b being the bifurcation parameter are plotted in Fig. 2. In each case 2001 parameter values filling uniformly the region of interest are selected. For each parameter value a trajectory of

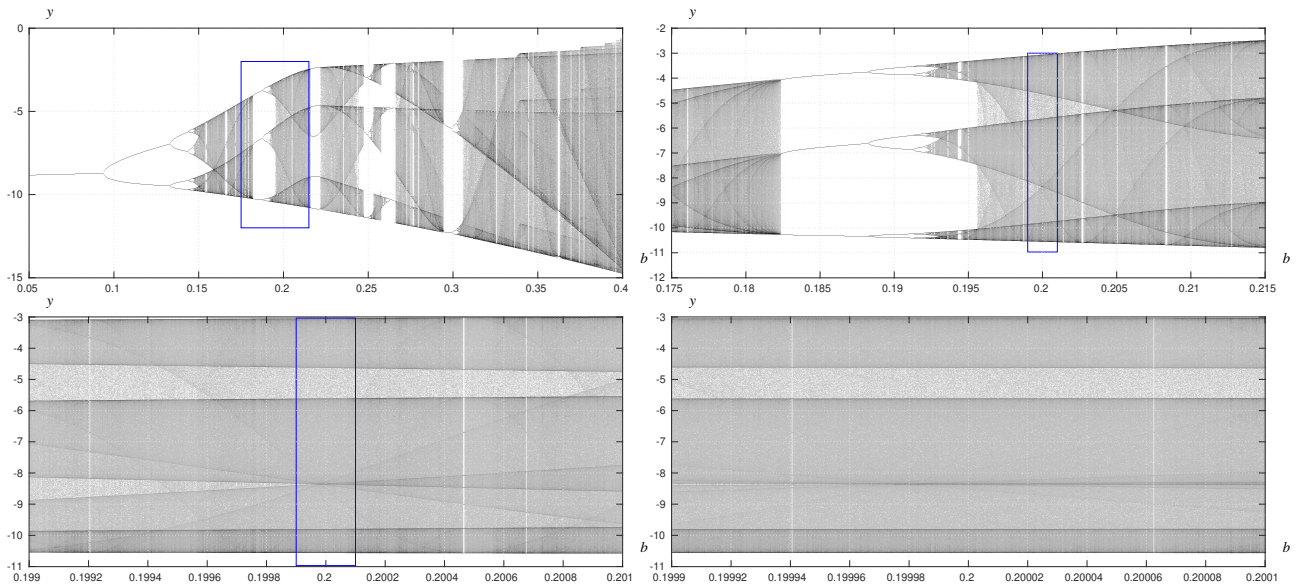


Figure 2: Bifurcation diagrams with b being the bifurcation parameter

the return map composed of 10000 points is computed. The first 5000 points are skipped and the remaining points are used to plot bifurcation diagrams. The y variable range is divided into 1000 bins and each bin is plotted with a grey level corresponding to the number of times a given bin was visited by the trajectory.

In the first case the parameter range is $b \in [0.05, 0.4]$. Several wide periodic windows can be easily identified. More detailed bifurcation diagrams are constructed for $b \in [0.175, 0.215]$, $b \in [0.199, 0.201]$, and $b \in [0.1999, 0.2001]$. The distance between sampling points for these three cases is $\Delta b = 2 \cdot 10^{-5}$, $\Delta b = 10^{-6}$, and $\Delta b = 10^{-7}$, respectively. For $b \in [0.175, 0.215]$ periodic attractors are observed for 545 parameter values (out of 2001), which corresponds to 30 periodic windows detected. Period-3 window enclosing the interval $b \in [0.18244, 0.18830]$ is the widest one. A period doubling cascade (period-6, period-12 and period-24 windows) originating from this periodic window can also be seen. In the last two cases only few narrow PWs may be identified (7 and 2, respectively).

Finding periodic windows by monitoring bifurcation diagrams permits detection of relatively few PWs only. First, to detect a periodic window we have to select a parameter value belonging to this window. It means that detection of narrow PWs requires very dense sampling of the parameter space. Practically, there is no chance to detect narrow windows with the width below 10^{-12} when the sampling distance is $\Delta b = 10^{-7}$ which is used in the case $b \in [0.1999, 0.2001]$ and 2001 sampling points. We show that the method presented in this work is capable of finding periodic windows with the widths below $2 \cdot 10^{-20}$. Second, for narrow windows the convergence time to the corresponding attractor is usually very large (compare [20]). In consequence, very long trajectories must be computed to obtain convergence and to find a periodic attractor.

Bifurcation diagrams with a being the bifurcation parameter are plotted in Fig. 3. Four cases are considered: $a \in [2, 10]$, $a \in [5.6, 5.8]$, $a \in [5.69, 5.71]$, $a \in [5.699, 5.701]$. 14 periodic windows are detected in $[5.6, 5.8]$. The widest is the period-7 window observed for $a \in [5.7643, 5.7654]$. Three PWs are detected for $a \in [5.69, 5.71]$. In the last case no PWs are found. It may seem that for $a \in [5.699, 5.701]$ the system is chaotic. In the following sections, we show that this is not true, and there are thousands of narrow periodic windows in this interval.

3.1 Symbolic dynamics based method to find periodic windows

In this section an efficient method to find periodic windows is presented. We assume that all parameters of the system are fixed apart from a single parameter μ which is called the bifurcation parameter. The problem is to find PWs of the return map P_μ in the interval $\mu \in [\mu_{\min}, \mu_{\max}]$. We assume that trajectories observed for the endpoints of $\mu \in [\mu_{\min}, \mu_{\max}]$ are chaotic.

Let us select $\mu \in [\mu_{\min}, \mu_{\max}]$ and let $(v_k)_{k=0}^{N-1}$ be a long numerically generated trajectory of the return map P_μ . In the first step, using the symbolic dynamics based method UPOs of P_μ are found (see [21] for a detailed description). Let us briefly recall this approach. First, the state space is divided in m regions and a point v_k belonging to the trajectory $(v_k)_{k=0}^{N-1}$ is assigned a symbol $s_k \in \{0, 1, \dots, m-1\}$, which is the index

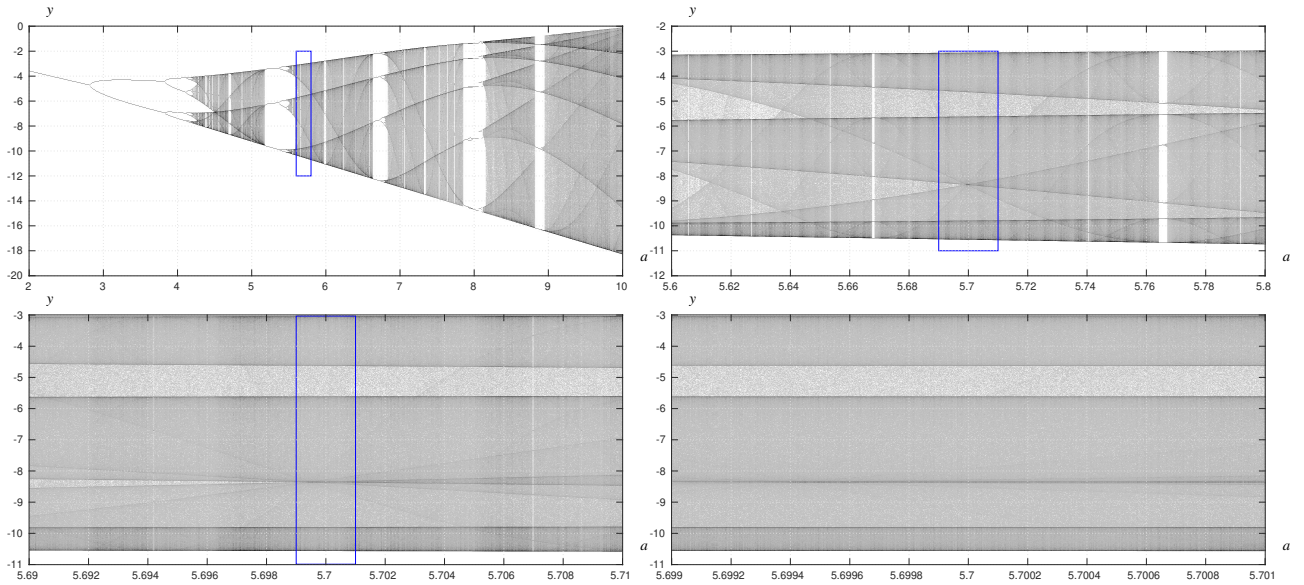


Figure 3: Bifurcation diagrams with a being the bifurcation parameter

of the region to which it belongs. The state space is divided into region corresponding to different symbols based on the plot of a single variable versus its previous iterate. Extreme values of the obtained plot are used to split the state space. In this study we use the variable y for this task. The plots of y_{k+1} versus y_k have a single extremum which is a minimum and in consequence the number of symbols is $m = 2$. We say that $(v_k)_{k=0}^{p-1}$ is a periodic orbit of P_μ with the (minimal) period p if $P_\mu(v_k) = v_{(k+1) \bmod p}$ for $k = 0, 1, \dots, p-1$ and $P_\mu(v_k) \neq v_0$ for any non-negative $k < p-1$. To find period- p orbits we consider all cyclically different symbol sequences $s = (s_k)_{k=0}^{p-1}$ with the (minimal) period p . For each symbol sequence s we construct an initial guess $\tilde{w} = (\tilde{u}_0, \tilde{u}_1, \dots, \tilde{u}_{p-1})$ of the position of an UPO with this symbol sequence. The construction is found using the symbol sequence representation of the trajectory $(v_k)_{k=0}^{N-1}$ (for details see [21]). The initial guess \tilde{w} is then used as an initial point for the Newton method. The Newton operator

$$N(w) = w - (F'(w))^{-1} F(w). \quad (2)$$

is applied to the map F defined by

$$F \begin{pmatrix} u_0 \\ u_1 \\ \dots \\ u_{p-1} \end{pmatrix} = \begin{pmatrix} P_\mu(u_0) - u_1 \\ P_\mu(u_1) - u_2 \\ \dots \\ P_\mu(u_{p-1}) - u_0 \end{pmatrix}. \quad (3)$$

It is clear that if $F(w) = 0$, where $w = (u_0, u_1, \dots, u_{p-1})$, then $P_\mu^p(u_0) = u_0$, which means that w is a periodic orbit of P_μ . Successive iterations of the Newton operator are calculated to obtain an accurate position \bar{w} of the orbit. When the Newton method converges we may hope that there exist a true periodic orbit in a neighborhood of the obtained result. The number of period- p symbol sequences to be considered may be reduced by excluding forbidden (unobserved) symbol sequences, which are identified by monitoring the trajectory $(v_k)_{k=0}^{N-1}$. Examples are shown in the following sections. The calculations described above are repeated for both endpoints μ_{\min} and μ_{\max} . In this way we obtain positions of UPOs for the maps $P_{\mu_{\min}}$ and $P_{\mu_{\max}}$ which serve as starting points for the continuation method to find PWs in the interval $\mu \in [\mu_{\min}, \mu_{\max}]$.

Next, the continuation method is applied for each UPO to find PWs in $\mu \in [\mu_{\min}, \mu_{\max}]$ [20]. We start at $\mu = \mu_{\min}$ or $\mu = \mu_{\max}$ and change μ to move along the interval $[\mu_{\min}, \mu_{\max}]$. After each parameter change the position of the orbit for new parameter value is found using the Newton method. If the Newton method converges then the parameter change is accepted. Otherwise, it is not accepted, the step $\Delta\mu$ is decreased and computations are repeated. This process is carried out until a stable periodic orbit is found, or the parameter μ is outside the interval $\mu \in [\mu_{\min}, \mu_{\max}]$, or the step $\Delta\mu$ is smaller than a predefined minimal value. When a periodic attractor is found the continuation method is used to find endpoints of the periodic window.

To prove the existence of a PW containing the parameter value μ we need to prove that the return map P_μ supports a periodic attractor. Let us denote by \bar{w} an approximate position of a periodic orbit of P_μ . To prove

the existence of a periodic orbit in a neighborhood of $\bar{w} = (\bar{u}_0, \bar{u}_1, \dots, \bar{u}_{p-1})$ we may use the interval Newton operator [22] defined as

$$N(\mathbf{w}, \bar{w}) = \bar{w} - (F'(\mathbf{w}))^{-1} F(\bar{w}), \quad (4)$$

where $\mathbf{w} = (\mathbf{u}_0, \mathbf{u}_1, \dots, \mathbf{u}_{p-1})$ is an interval vector containing \bar{w} . To carry out the existence proof one selects a narrow interval vector \mathbf{w} centered at \bar{w} and verifies the condition $N(\mathbf{w}, \bar{w}) \subset \mathbf{w}$. If this condition is satisfied then there exist a single zero of F in \mathbf{w} (compare [22]). In case the existence condition does not hold one may inflate the interval vector \mathbf{w} and repeat the computation. To prove that the periodic orbit is stable it is sufficient to show that bounds of eigenvalues of the Jacobian matrix $(P^p)'(\mathbf{u}_0) = P'(\mathbf{u}_{p-1}) \cdots P'(\mathbf{u}_1)P'(\mathbf{u}_0)$ are enclosed in the unit circle.

3.2 Primary and period-tupling windows

In the following, we consider the case when the return map is approximately equivalent to a one-dimensional map $f: I \ni y \mapsto f(y) \in I$ with a single extremum, which is a minimum. This is the case observed for the Rössler system in the region of interest. In this case one may use certain properties of underlying symbolic dynamics to eliminate certain symbol sequences from the search procedure and to select symbol sequences corresponding to wide periodic windows. Let us introduce several notions which are necessary to describe this procedure. We follow the notations used in [3, 7, 23–25]. We assume that the minimum of f is at $y = y_{ts}$. To a trajectory (y_k) of f we associate the symbol sequence s_k satisfying conditions $s_k = 1$ when $y_k < y_{th}$ and $s_k = 0$ otherwise. Note that the symbol assignment is different than for the logistic map (compare [25]), where the symbol $s_k = 0$ is assigned to points with $y_k < y_{th}$. This difference is caused by the fact that in our case the map f has a single minimum, while for the logistic map a single maximum exists.

Period- p orbit $(y_0, y_1, \dots, y_{p-1})$ corresponds to a symbol sequence $s = (s_0, s_1, \dots, s_{p-1})$ with the (minimum) period p . We say that a periodic sequence $s = (s_0, s_1, \dots, s_{p-1})$ is *odd-parity* (*even-parity*) if the sum $\sum_{k=0}^{p-1} s_k$ is an odd number (even number). Let us introduce the ordering ‘ \prec ’ in the set of symbol sequences (see also [7]). We say that $s \prec t$ if $s_k < t_k$ and $\sum_{j=0}^{k-1} s_j$ is even or $s_k > t_k$ and $\sum_{j=0}^{k-1} s_j$ is odd, where k is the smallest index such that $s_k \neq t_k$. We say that a period- p sequence $s = (s_0, s_1, \dots, s_{p-1})$ is *minimal* if none of its cyclic permutations is smaller than s according to the ordering ‘ \prec ’. Each minimal sequence must start with the number of zeros not smaller than the number of initial zeros of its cyclic permutations. For example the sequence $s = (0010101)$ is minimal since its permutation starts either with 1 or with 01 and it is clear that $(0010101) \prec (1\dots)$ and $(0010101) \prec (01\dots)$. In case of minimal periodic sequences the ordering ‘ \prec ’ has an important property that it agrees with the ordering of corresponding periodic windows in the parameter space. Two minimal periodic sequences with different periods can be compared by first converting each of them to the corresponding infinitely long symbol sequence in the following way $s = (s_0, s_1, \dots, s_{p-1}) = (s_0, s_1, \dots, s_{p-1}, s_0, s_1, \dots, s_{p-1}, \dots)$.

Let $s = (s_0, s_1, s_2, \dots, s_{p-2}, s_{p-1})$ be a period- p odd-parity minimal symbol sequence. The sequence $\bar{s} = (s_0, s_1, \dots, s_{p-3}, 1 - s_{p-2}, s_{p-1})$ which differs from s only at the second to last position is called an *even-parity partner of s* if it has the (minimal) period equal to p . A period- p odd-parity minimal symbol sequence s which has an even-parity partner \bar{s} is called a *saddle-node* sequence. Saddle-node sequences and their even-parity partners correspond to periodic orbits created via a saddle-node bifurcation. A period- p odd-parity minimal symbol sequence $s = (s_0, s_1, s_2, \dots, s_{p-3}, s_{p-2}, s_{p-1})$ with no even-parity partner (the sequence \bar{s} has the (minimal) period smaller than p) is called a *period-doubling sequence*. Such sequences correspond to periodic orbits created via a period-doubling bifurcation. The names for saddle-node and period-doubling sequences are derived from the type of bifurcation to which they lead.

Let s be a saddle-node sequence with the period- p and \bar{s} its even-parity partner. Let us select $n \geq 2$ and an odd integer $n_1 < n$. The sequence t obtained by concatenation of n_1 copies of s and $n_2 = n - n_1$ copies of \bar{s} is called a *period- n -tupling* sequence generated from s . From the fact that n_1 is odd it follows that the sequence t is an odd-parity sequence. A period-doubling sequence $t = (s, \bar{s})$ is a special case of a period-tupling sequence with $n_1 = 1$ and $n = 2$. For each saddle-node sequence s there exist a single period-tripling sequence $t = (s, \bar{s}, \bar{s})$ ($n_1 = 1$), and two period-quadrupling sequences: $t = (s, \bar{s}, \bar{s}, \bar{s})$ with $n_1 = 1$, $t = (s, \bar{s}, s, s)$ with $n_1 = 3$. We will use the following notation to define period-tupling sequences. Let s be a saddle-node sequence and t be an odd-parity sequence with the period n . s^t denotes the period- n -tupling sequence $s^t = (\delta(t_0), \delta(t_1), \dots, \delta(t_{n-1}))$, where $\delta(t_k) = s$ if $t_k = 1$ and $\delta(t_k) = \bar{s}$ otherwise. For example for $s = (0010101)$, $\bar{s} = (0010111)$ and $t = (100)$ we obtain $s^t = s^{(100)} = (s, \bar{s}, \bar{s}) = (0010101 0010111 0010111)$. Sequences, which are not period-tupling sequences are called *primary* sequences. PWs corresponding to primary and period-tupling sequences are called *primary* and *period-tupling* windows, respectively. In the following, we show that period-tupling

windows are usually much wider than primary windows with the same period. Thus, study of period-tupling windows is essential in obtaining accurate approximations of the total width of periodic windows.

4 Periodic windows for the Rössler system close to the classical case

In this section, the existence of periodic windows for the Rössler system close to the classical parameter values $(a, b) = (5.7, 0.2)$ is studied. We find PWs existing in the regions $(a, b) \in [5.6, 5.8] \times \{0.2\}$ and $(a, b) \in \{5.7\} \times [0.175, 0.215]$ using the approach presented in Section 3. Let us first consider the case $a \in [5.6, 5.8]$, $b = 0.2$.

4.1 Periodic windows for $a \in [5.6, 5.8]$, $b = 0.2$

In the first step UPOs existing for $a \in \{5.6, 5.7, 5.8\}$ and $b = 0.2$ are found. For each case a trajectory $(v_k)_{k=0}^{N-1}$ of $P_{a,b}$ with the length $N = 10^6$ is generated, the minimum value of y in the time series is found and its preimage is used to define the threshold value y_{th} for the symbolic dynamics representation. Threshold values used to split the attractor are $y_{\text{th}} = -6.6412775$, $y_{\text{th}} = -6.73872$, and $y_{\text{th}} = -6.836085$ for $a = 5.6$, $a = 5.7$, and $a = 5.8$, respectively (compare Fig. 4).

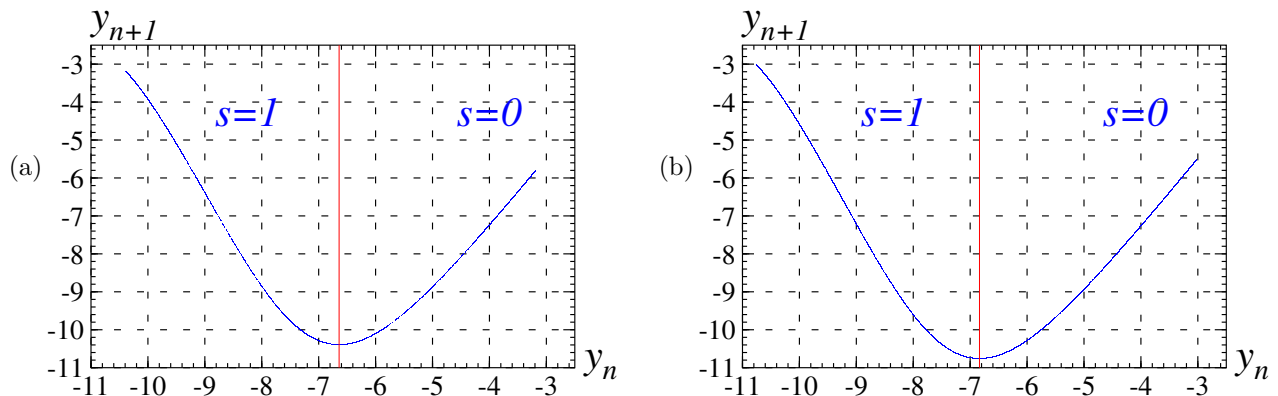


Figure 4: Symbolic representations of trajectories of P ; (a) $a = 5.6$, $b = 0.2$, the threshold value $y_{\text{th}} = -6.6412775$, (b) $a = 5.8$, $b = 0.2$, the threshold value $y_{\text{th}} = -6.836085$.

For $a = 5.6$ the following short sequences of the length $l \leq 12$ are not observed in the trajectory $(v_k)_{k=0}^{N-1}$: (000), (0011), (001010), (0010111), (001011010), (0010110111). These sequences are called forbidden and are excluded in the search for unstable periodic orbits. Note that the so-called forbidden sequences found are not proved to be forbidden, they are just not observed in the computer generated trajectory $(v_k)_{k=0}^{N-1}$. In consequence, the elimination procedure (skipping forbidden sequences) may remove some admissible (non-forbidden) sequences which are rarely observed in a chaotic trajectory. To reduce this risk one should consider a trajectory significantly longer than $2^{l_{\text{max}}}$, where l_{max} is the maximum length of a forbidden symbol sequence which we search for. We use $l_{\text{max}} = 12$ and trajectories of the length $N = 10^6 > 4096 = 2^{12}$. All cyclically different symbol sequences with periods $p \leq 27$ not containing forbidden sequences are generated. There are $S_{\text{nf}} = 51676$ such sequences. For each symbol sequence a candidate of the corresponding periodic orbit is constructed. An accurate approximation of the periodic orbit position is found by applying the Newton method. Convergence of the Newton method indicates that there may exist a periodic orbit in a neighborhood of the position found by the Newton method. The convergence is observed in case of $P_{\leq 27} = 50233$ symbol sequences out of $S_{\text{nf}} = 51676$ non-forbidden sequences.

Next, the interval Newton operator (4) is applied to prove the existence of periodic orbits. This procedure is successful in case of 50045 periodic orbits when calculations were carried out using double-precision interval computations. For the remaining 188 orbits the calculations are carried out using multiprecision computations with the GNU MPFR library [19]. All the periodic orbits found are unstable, which is verified by computing bounds of eigenvalues of the Jacobian matrix of $P_{a,0.2}^p$ over the verified enclosure of a period- p orbit of P . If at least one eigenvalue lies outside the unit circle then the orbit is unstable. This condition is verified for all periodic orbits. At a final step, we confirm that all UPOs found are different. This is achieved by verifying that intervals being rigorous bounds of periodic orbits flow times are pairwise disjoint. Summarizing, we proved

that the number of UPOs with the periods $p \leq 27$ is not less than $P_{\leq 27} = 50233$. We would like to stress that this is a lower bound. There may exist periodic orbits which are not detected by the search procedure. One of the reasons may be that the Newton method does not converge or converges to a periodic orbit with a different symbol sequence. Another reason may be excluding some admissible sequences in the process of finding forbidden sequences. However, it was shown in [21] that the symbolic dynamics based search method is successful in locating all periodic orbits with periods $p \leq 20$ for classical parameter values $a = 5.7$, $b = 0.2$. Thus, we may hope that the majority (perhaps all) of periodic orbits with periods $p \leq 27$ have been found.

Note that the total number of cyclically different symbol sequences with periods $p \leq 27$ is $S_{\text{all}} = 10358999$ and the number of admissible (non-forbidden) symbol sequences is $S_{\text{nf}} = 51676$. This shows that eliminating forbidden sequences significantly reduces the computation time. Let us also note that the number $P_{\leq 27} = 50233$ of cycles found is only slightly smaller than the number $S_{\text{nf}} = 51676$ of symbol sequences considered, which indicates that the elimination procedure is successful.

For $a = 5.8$ the forbidden sequences of the length $p \leq 12$ are (000), (0011), (0010100), (00101011), (0010101010), (00101010111). In this case there are $S_{\text{nf}} = 138298$ cyclically different non-forbidden symbol sequences with periods $p \leq 27$ and they lead to $P_{\leq 27} = 134631$ periodic orbits. Their existence and stability properties are proved by applying the interval Newton method implemented in double precision (134225 cases) and multiple precision (406 cases) interval arithmetic.

The numbers P_p of unstable period- p orbits found for endpoints and the midpoint of the interval $(a, b) \in [5.6, 5.8] \times \{0.2\}$ are given in Table 1. We also report the number Q_p of fixed points of the p th iterate of the return map $P_{a,0.2}$, which can be computed using the formula $Q_p = \sum_{k=1, p \bmod k=0}^{p-1} k P_k$.

Table 1: The numbers P_p of unstable period- p orbits found, the numbers Q_p of fixed points of $P_{a,b}^p$, and estimates H_p of the topological entropy of $P_{a,0.2}$ based on Q_p , $(a, b) \in \{5.6, 5.7, 5.8\} \times \{0.2\}$.

p	$a = 5.6, b = 0.2$			$a = 5.7, b = 0.2$			$a = 5.8, b = 0.2$		
	P_p	Q_p	H_p	P_p	Q_p	H_p	P_p	Q_p	H_p
1	1	1	0.00000	1	1	0.00000	1	1	0.00000
2	1	3	0.54931	1	3	0.54931	1	3	0.54931
3	2	7	0.64864	2	7	0.64864	2	7	0.64864
4	1	7	0.48648	1	7	0.48648	1	7	0.48648
5	2	11	0.47958	2	11	0.47958	2	11	0.47958
6	3	27	0.54931	3	27	0.54931	3	27	0.54931
7	4	29	0.48104	4	29	0.48104	6	43	0.53731
8	5	47	0.48127	7	63	0.51789	7	63	0.51789
9	10	97	0.50830	10	97	0.50830	12	115	0.52721
10	11	123	0.48122	15	163	0.50938	19	203	0.53132
11	18	199	0.48121	24	265	0.50725	28	309	0.52121
12	28	367	0.49211	36	463	0.51148	42	535	0.52352
13	42	547	0.48496	58	755	0.50975	72	937	0.52636
14	60	871	0.48355	88	1263	0.51009	105	1515	0.52308
15	100	1517	0.48830	138	2087	0.50957	172	2597	0.52414
16	143	2335	0.48474	216	3519	0.51037	272	4415	0.52455
17	222	3775	0.48448	340	5781	0.50955	434	7379	0.52391
18	343	6291	0.48594	531	9675	0.50985	684	12447	0.52385
19	528	10033	0.48493	848	16113	0.50986	1112	21129	0.52413
20	806	16247	0.48478	1330	26767	0.50975	1770	35607	0.52401
21	1270	26705	0.48536	2120	44555	0.50974	2858	60067	0.52396
22	1947	43035	0.48499	3364	74275	0.50980	4604	101599	0.52404
23	3034	69783	0.48492	5368	123465	0.50973	7458	171535	0.52402
24	4731	113951	0.48515	8551	205743	0.50977	12034	289407	0.52398
25	7378	184461	0.48501	13698	342461	0.50976	19562	489061	0.52401
26	11493	299367	0.48498	21899	570131	0.50975	31732	825971	0.52401
27	18050	487447	0.48507	35154	949255	0.50976	51638	1394341	0.52400
≤ 27	50233	1265565	0.48507	93809	2374821	0.50976	134631	3416769	0.52400

As a byproduct of these computation we may compute estimates $H_p = p^{-1} \log Q_p$ of the topological entropy of $P_{a,0.2}$ based on the number Q_p of fixed points of $P_{a,0.2}^p$. Note that these estimates stabilize quite fast and that three most significant digits of these estimates do not change for $p \geq 20$. One may also see that the complexity of $P_{a,0.2}$ measured in terms of the topological entropy grows from 0.485 to 0.524 when the parameter a is increased

from $a = 5.6$ to $a = 5.8$.

In the second step of the procedure to find PWs in the interval $a \in [5.6, 5.8]$ we continue periodic orbits found for the endpoints $a = 5.6$ and $a = 5.8$ within the interval $a \in [5.6, 5.8]$. It is expected that a PW with the specific symbol sequence s exists in the interval $a \in [5.6, 5.8]$ only if this sequence is admissible for exactly one of the endpoints of this interval. This is related to the fact that the plots of y_{k+1} versus y_k for $a \in [5.6, 5.8]$, $b = 0.2$ are very close to plots of a one-dimensional map with a single extremum and moreover that the complexity of the map measured in terms of the topological entropy changes monotonically when the parameter a is changed. For such maps (a good example is the logistic map) a stable periodic orbit is born via a saddle-node or period-doubling bifurcation for a certain parameter value, which is the first endpoint of the periodic window. At the second endpoint the orbit loses stability. However, further modifications of the parameter do not make the orbit disappear as this would require another bifurcation and this scenario is not observed for such systems. The property that a periodic window associated with a given symbol sequence exists only if this sequence is admissible for exactly one of the endpoints is confirmed by continuing orbits found for $a = 5.6$. Each periodic orbit existing for $a = 5.6$ could be continued past the point $a = 5.8$ and in consequence no PWs in the interval $a \in [5.6, 5.8]$ are detected. This is in full agreement with the fact that all sequences admissible for $a = 5.6$ are also admissible for $a = 5.8$. Continuation of periodic orbits found for $a = 5.8$ leads to $W_{\leq 27} = 42216$ periodic windows. Their existence is confirmed by applying the interval Newton method to prove the existence of a periodic orbit for a parameter value belonging to the periodic window and proving that the orbit is stable by verifying that the dominant eigenvalue (with the maximum absolute value) of the corresponding Jacobian matrix is smaller than one in absolute value. Widths of PWs are estimated using the continuation method. For each PW we locate two points being close to endpoints of the PW for which the (non-rigorous) Newton method converges to a stable periodic orbit. These results are not rigorous. The distance between these two points is used as a non-rigorous lower bound on the periodic window width. In case of narrow periodic windows all the calculations are carried out in multiple precision. This includes the continuation procedure to find a parameter value belonging to the periodic window and also the calculations involving the interval Newton operator to prove the existence of a periodic attractor.

During these computations it is confirmed that it is sufficient to consider odd-parity sequences only. Even-parity sequences do not lead to new PWs. As an example let us consider two period-7 symbol sequences which are admissible for $a = 5.8$ and are not admissible for $a = 5.6$. $s = (0010101)$ is an odd-parity sequence and $\bar{s} = (0010111)$ is its even-parity partner. Dominant eigenvalues of the Jacobian matrices of $P_{a,0.2}^7$ computed along the continued periodic orbits are plotted in Fig. 5. The orbit is stable when the dominant eigenvalue satisfies the condition $|\lambda| < 1$. One can see that the odd-parity sequence $s = (0010101)$ leads to a PW while the even-parity sequence $\bar{s} = (0010111)$ leads to a saddle-node bifurcation points where two period-7 orbits are born.

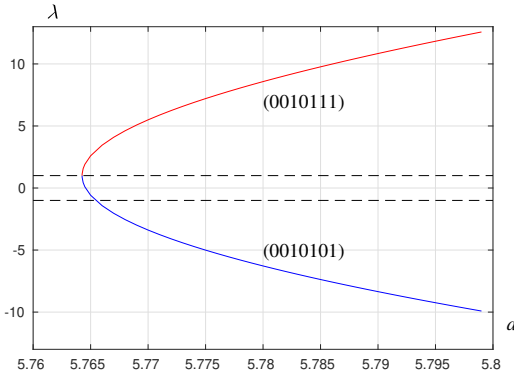


Figure 5: The dominant eigenvalue of the Jacobian matrix of $P_{a,0.2}^7$ computed along period-7 orbits versus the bifurcation parameter a .

The results regarding the number of periodic windows and their widths are reported in Table 2. W_p denotes the number of period- p windows found, and w_p is their total width. We also report the number $W_{p,PR}$ and the total width $w_{p,PR}$ of period- p primary windows. In total, $W_{\leq 27} = 42216$ PWs with periods $p \leq 27$ are found and their total width is $w_{\leq 27} \approx 3.064 \cdot 10^{-3}$. The widest one is the period-7 window with the symbol sequence $s = (0010101)$ and the width $w \approx 1.188 \cdot 10^{-3}$. The narrowest PW found have widths below 10^{-18} .

Note that for each $p \leq 27$ the number $2 \cdot (W_p - W_{p,PD}) + W_{p,PD}$ is equal to the difference between the

Table 2: Period windows existing for $(a, b) \in [5.6, 5.8] \times \{0.2\}$, W_p is the number of period- p windows found, w_p is the total width of period- p windows, $W_{p,PR}$ and $w_{p,PR}$ are the number and the total width of primary period- p windows found, $W_{p,PD}$ is the number of period-doubling windows found

p	W_p	w_p	$w_{p,\max}$	$W_{p,PR}$	$w_{p,PR}$	$w_{p,PR,\max}$	$W_{p,PD}$
7	1	$1.188 \cdot 10^{-3}$	$1.188 \cdot 10^{-3}$	1	$1.188 \cdot 10^{-3}$	$1.188 \cdot 10^{-3}$	0
8	1	$3.493 \cdot 10^{-4}$	$3.493 \cdot 10^{-4}$	1	$3.493 \cdot 10^{-4}$	$3.493 \cdot 10^{-4}$	0
9	1	$4.646 \cdot 10^{-5}$	$4.646 \cdot 10^{-5}$	1	$4.646 \cdot 10^{-5}$	$4.646 \cdot 10^{-5}$	0
10	4	$2.245 \cdot 10^{-4}$	$9.284 \cdot 10^{-5}$	4	$2.245 \cdot 10^{-4}$	$9.284 \cdot 10^{-5}$	0
11	5	$8.916 \cdot 10^{-5}$	$4.563 \cdot 10^{-5}$	5	$8.916 \cdot 10^{-5}$	$4.563 \cdot 10^{-5}$	0
12	7	$1.548 \cdot 10^{-5}$	$4.685 \cdot 10^{-6}$	7	$1.548 \cdot 10^{-5}$	$4.685 \cdot 10^{-6}$	0
13	15	$5.553 \cdot 10^{-5}$	$1.863 \cdot 10^{-5}$	15	$5.553 \cdot 10^{-5}$	$1.863 \cdot 10^{-5}$	0
14	23	$6.252 \cdot 10^{-4}$	$5.952 \cdot 10^{-4}$	22	$3.002 \cdot 10^{-5}$	$1.320 \cdot 10^{-5}$	1
15	36	$6.014 \cdot 10^{-6}$	$1.142 \cdot 10^{-6}$	36	$6.014 \cdot 10^{-6}$	$1.142 \cdot 10^{-6}$	0
16	65	$1.884 \cdot 10^{-4}$	$1.737 \cdot 10^{-4}$	64	$1.467 \cdot 10^{-5}$	$2.443 \cdot 10^{-6}$	1
17	106	$1.352 \cdot 10^{-5}$	$2.510 \cdot 10^{-6}$	106	$1.352 \cdot 10^{-5}$	$2.510 \cdot 10^{-6}$	0
18	171	$2.543 \cdot 10^{-5}$	$2.326 \cdot 10^{-5}$	170	$2.176 \cdot 10^{-6}$	$1.755 \cdot 10^{-7}$	1
19	292	$4.882 \cdot 10^{-6}$	$4.081 \cdot 10^{-7}$	292	$4.882 \cdot 10^{-6}$	$4.081 \cdot 10^{-7}$	0
20	484	$1.169 \cdot 10^{-4}$	$4.618 \cdot 10^{-5}$	480	$4.678 \cdot 10^{-6}$	$5.487 \cdot 10^{-7}$	4
21	794	$2.253 \cdot 10^{-5}$	$2.174 \cdot 10^{-5}$	793	$7.878 \cdot 10^{-7}$	$3.230 \cdot 10^{-8}$	0
22	1331	$4.639 \cdot 10^{-5}$	$2.290 \cdot 10^{-5}$	1326	$1.779 \cdot 10^{-6}$	$1.515 \cdot 10^{-7}$	5
23	2212	$1.688 \cdot 10^{-6}$	$1.130 \cdot 10^{-7}$	2212	$1.688 \cdot 10^{-6}$	$1.130 \cdot 10^{-7}$	0
24	3655	$1.471 \cdot 10^{-5}$	$6.479 \cdot 10^{-6}$	3647	$4.881 \cdot 10^{-7}$	$5.894 \cdot 10^{-8}$	7
25	6092	$6.414 \cdot 10^{-7}$	$2.550 \cdot 10^{-8}$	6092	$6.414 \cdot 10^{-7}$	$2.550 \cdot 10^{-8}$	0
26	10127	$2.834 \cdot 10^{-5}$	$9.325 \cdot 10^{-6}$	10112	$5.783 \cdot 10^{-7}$	$2.377 \cdot 10^{-8}$	15
27	16794	$1.158 \cdot 10^{-6}$	$8.596 \cdot 10^{-7}$	16793	$2.980 \cdot 10^{-7}$	$2.705 \cdot 10^{-8}$	0
≤ 27	42216	$3.064 \cdot 10^{-3}$	$1.188 \cdot 10^{-3}$	42179	$2.051 \cdot 10^{-3}$	$1.188 \cdot 10^{-3}$	34
28–224	843	$3.910 \cdot 10^{-4}$	$1.404 \cdot 10^{-4}$	0	0	0	464
all	43059	$3.455 \cdot 10^{-3}$	$1.188 \cdot 10^{-3}$	42179	$2.051 \cdot 10^{-3}$	$1.188 \cdot 10^{-3}$	498

number of UPOs found for $a = 5.8$ and $a = 5.6$. For example for $p = 24$ we have $W_p = 3655$, $W_{p,PD} = 7$, $2 \cdot (W_p - W_{p,PD}) + W_{p,PD} = 7303$ and $P_p(a = 5.8) - P_p(a = 5.6) = 12034 - 4731 = 7303$. This is due to the following facts: (i) all sequences admissible for $a = 5.6$ are also admissible for $a = 5.8$, (ii) period-doubling sequences admissible only for $a = 5.8$ lead to period-doubling windows (such sequences do not have even-parity partners), and (iii) half of the remaining sequences admissible only for $a = 5.8$ lead to saddle-node windows (the other half are their even-parity partners which do not produce new PWs). There is no case in which only one periodic orbit was detected for a pair of a saddle-node sequence and its even-parity partner. These observations further confirm that the symbolic dynamics approach permits finding all UPOs with a given period. The results obtained also show that the continuation method works fine for small periods (a PW is found for each even parity symbol sequence admissible only for one endpoint of the bifurcation interval). It is interesting to observe that for even p the number $W_{p,PD}$ of period-doubling windows is the same as the number $W_{p/2}$ of periodic windows found for the period $p/2$. This means that all period-doubling bifurcations are correctly detected.

Let us note that for periods for which period-tupling windows exist ($W_{p,PR} < W_p$) those PWs have a significant impact on the total window width w_p . As an example let us consider the case $p = 14$ where the number of primary windows is $W_{14,PR} = 22$ and the total number of windows is $W_{14} = 23$. The only period-tupling window has the width $w_{14,\max} \approx 5.952 \cdot 10^{-4}$ while the total width of period-14 primary windows is almost twenty times smaller $w_{14,PR} \approx 3.002 \cdot 10^{-5}$. For $p = 16$ the width of the only period-tupling window $w_{16,\max} \approx 1.737 \cdot 10^{-4}$ is more than 10 times larger than the total width of all 64 period-16 primary windows $w_{16,PR} \approx 1.467 \cdot 10^{-5}$. Similar results are observed for larger periods. It follows that period-tupling windows have dominant influence on the total width of period- p windows for large p . Let us also note that primary windows with periods $p \in \{25, 26, 27\}$ have widths below $3 \cdot 10^{-8}$. Thus, one may expect that there are very few (if any) primary windows with periods $p \geq 28$ and widths above $3 \cdot 10^{-8}$.

In order to improve the lower bound $w_{\leq 27} \approx 3.064 \cdot 10^{-3}$ of the total width of PWs we look for wide period-tupling windows with periods $p \geq 28$. First, period-tupling sequences generated from the shortest primary sequence $s = (0010101)$ are constructed and corresponding period-tupling windows are found. This procedure leads to 81 period-tupling windows with periods $28 \leq p \leq 210$ and the total width of $2.112 \cdot 10^{-4}$. Similar computations are carried out for other primary windows with periods $p \leq 27$. In this way 843 period-tupling windows with periods $28 \leq p \leq 224$ and the total width of $3.91 \cdot 10^{-4}$ are found. The three widest period-tupling

windows correspond to symbol sequences: $(0010101)^{(1011)}$, $(00101111)^{(1011)}$, $(0010101)^{(10111010)}$ with periods 28, 32, and 56. Their widths are $1.404 \cdot 10^{-4}$, $4.1 \cdot 10^{-5}$, and $3.084 \cdot 10^{-5}$, respectively.

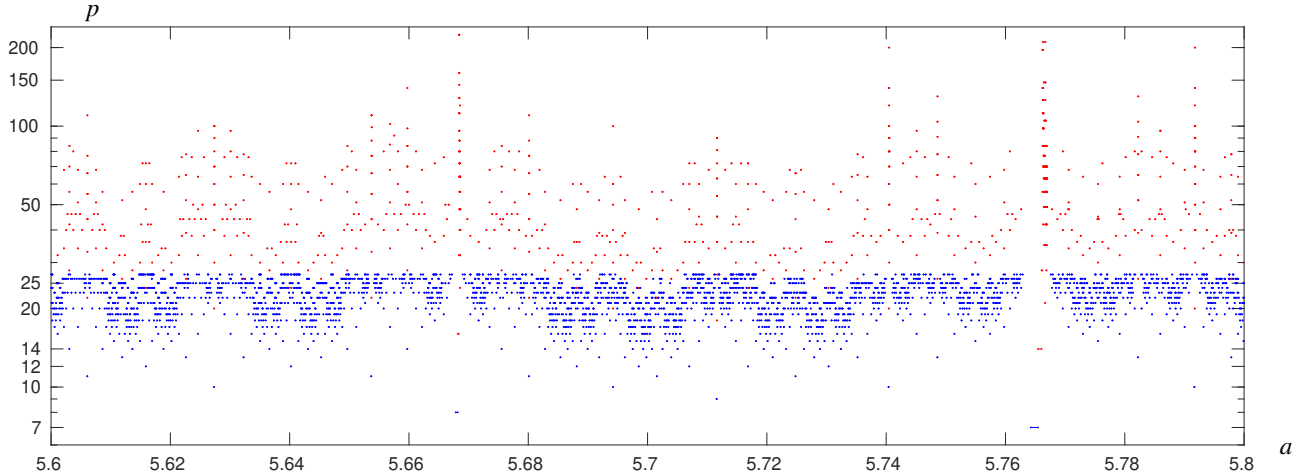


Figure 6: Periodic windows with the width above 10^{-10} found in the region $a \in [5.6, 5.8]$, $b = 0.2$. Primary and period-tupling windows are plotted in blue and red, respectively.

Periodic windows found are plotted in Fig. 6. Results regarding primary and period-tupling windows are plotted in blue and red, respectively. The total width of PWs found is $3.455 \cdot 10^{-3}$ which is approximately 1.73% of the width of the interval $a \in [5.6, 5.8]$. The closest periodic window to the classical case $a = 5.7$ is the period-27 window with the width $w \approx 4.22 \cdot 10^{-13}$. This periodic window contains the point $a = 5.699999143892$. Its distance from $a = 5.7$ is less than $8.57 \cdot 10^{-7}$. The maximum distance between periodic windows found is smaller than $1.4 \cdot 10^{-3}$, which indicates that PWs densely fill the interval $a \in [5.6, 5.8]$ (compare also Fig. 6).

4.2 Periodic windows for $a = 5.7$, $b \in [0.175, 0.215]$

Let us now consider the interval $(a, b) \in \{5.7\} \times [0.175, 0.215]$. The results concerning the number of periodic orbits with periods $p \leq 27$ found for $a = 5.7$ and $b \in \{0.175, 0.2, 0.215\}$ are reported in Table 3. There are $P_{\leq 27} = 28732$ and $P_{\leq 27} = 221219$ UPOs found for $b = 0.175$ and $b = 0.215$, respectively.

A systematic symbolic dynamics based procedure is applied to find PWs with periods $p \leq 27$. The results regarding the number of periodic windows and their widths are given in Table 4. $W_{\leq 27} = 96280$ periodic windows are found. Their total width is $w_{\leq 27} \approx 1.036 \cdot 10^{-2}$. The widest window has period $p = 3$ and the width $w \approx 5.894 \cdot 10^{-3}$. The narrowest window has period $p = 27$ and the width below $2 \cdot 10^{-20}$.

Additionally, we find 3567 period-tupling windows with periods $28 \leq p \leq 160$ and the total width $1.674 \cdot 10^{-4}$. Thus, the lower bound on the width of periodic windows in the interval $b \in [0.175, 0.215]$ can be estimated as $1.053 \cdot 10^{-2}$ which is approximately 26% of the width of the interval $[0.175, 0.215]$. The much larger coverage of the bifurcation region by periodic windows when compared to the case considered in Section 4.1 is caused by the presence of the wide period-3 window with the symbol sequence $s = (001)$ and its period-tupling descendants. The three widest period-tupling windows with periods above 28 correspond to symbol sequences: $(001)^{(1011101010111011)}$, $(001)^{(101111101110)}$, $(001)^{(10111010111)}$ with periods 48, 36, and 30. Their widths are $3.359 \cdot 10^{-5}$, $1.45 \cdot 10^{-5}$, and $1.122 \cdot 10^{-5}$, respectively.

Periodic windows are plotted in Fig. 7. The closest periodic window to the classical case is period-27 window with the width $1.69 \cdot 10^{-14}$ containing the point $b = 0.19999996572539$. Its distance from $b = 0.2$ is less than $3.5 \cdot 10^{-8}$. The second closest one is period-25 window with the width $1.14 \cdot 10^{-13}$. It contains the point $b = 0.2000000949446$ with the distance from $b = 0.2$ less than $9.5 \cdot 10^{-8}$. Periodic attractors existing for $b = 0.19999996572539$ and $b = 0.2000000949446$ are plotted in Fig. 8. Periodic windows densely fill the region $b \in [0.175, 0.215]$ —the maximum distance between periodic windows found is smaller than $7 \cdot 10^{-4}$ (compare Fig. 7).

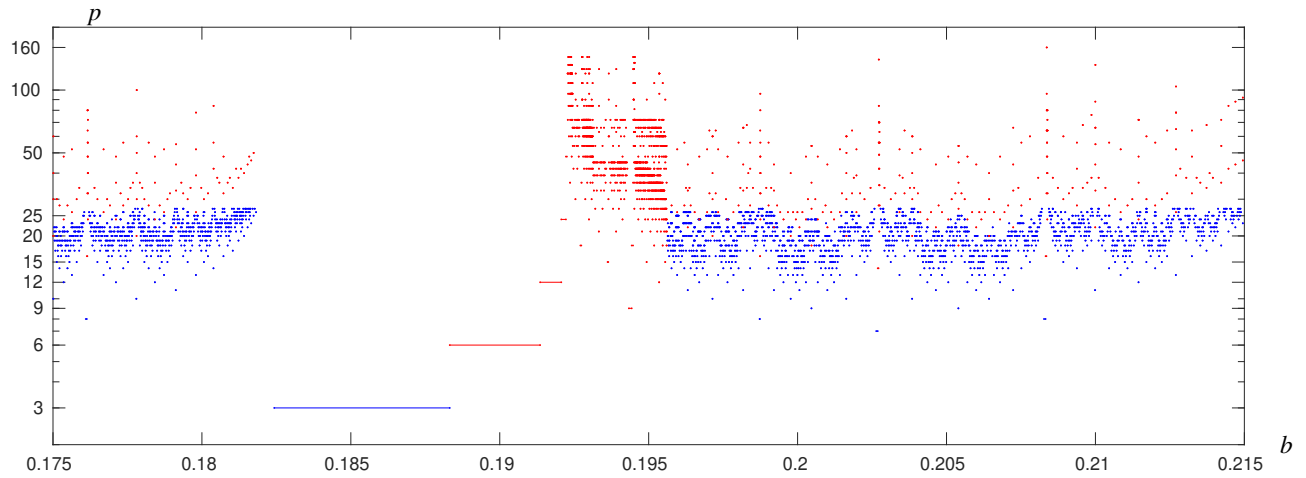


Figure 7: Periodic windows with the width above 10^{-10} found in the region $a = 5.7$, $b \in [0.175, 0.215]$. Primary and period-tupling windows are plotted in blue and red, respectively.

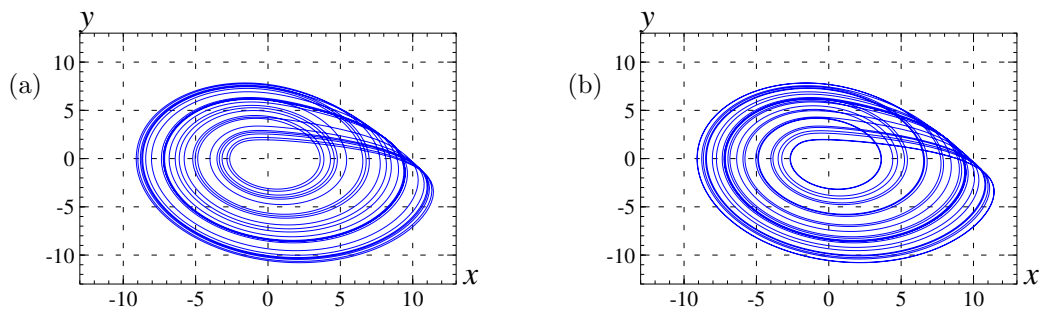


Figure 8: Periodic attractors of the Rössler system close to the classical case; (a) $a = 5.7$, $b = 0.2000000949446$, period $p = 25$, (b) $a = 5.7$, $b = 0.19999996572539$, period $p = 27$.

Table 3: The numbers P_p of unstable period- p orbits found, $(a, b) \in \{5.7\} \times \{0.175, 0.2, 0.215\}$.

p	$a = 5.7, b = 0.175$			$a = 5.7, b = 0.2$			$a = 5.7, b = 0.215$		
	P_p	Q_p	H_p	P_p	Q_p	H_p	P_p	Q_p	H_p
1	1	1	0.00000	1	1	0.00000	1	1	0.00000
2	1	3	0.54931	1	3	0.54931	1	3	0.54931
3	0	1	0.00000	2	7	0.64864	2	7	0.64864
4	1	7	0.48648	1	7	0.48648	1	7	0.48648
5	2	11	0.47958	2	11	0.47958	2	11	0.47958
6	2	15	0.45134	3	27	0.54931	3	27	0.54931
7	4	29	0.48104	4	29	0.48104	6	43	0.53731
8	3	31	0.42925	7	63	0.51789	9	79	0.54618
9	8	73	0.47672	10	97	0.50830	14	133	0.54337
10	7	83	0.44188	15	163	0.50938	21	223	0.54072
11	16	177	0.47056	24	265	0.50725	36	397	0.54399
12	19	247	0.45912	36	463	0.51148	54	679	0.54339
13	32	417	0.46408	58	755	0.50975	90	1171	0.54351
14	44	647	0.46231	88	1263	0.51009	141	2019	0.54360
15	68	1031	0.46255	138	2087	0.50957	230	3467	0.54340
16	102	1663	0.46352	216	3519	0.51037	369	5983	0.54354
17	152	2585	0.46220	340	5781	0.50955	606	10303	0.54354
18	228	4191	0.46337	531	9675	0.50985	977	17739	0.54353
19	344	6537	0.46238	848	16113	0.50986	1608	30553	0.54354
20	522	10527	0.46308	1330	26767	0.50975	2619	52607	0.54353
21	788	16577	0.46266	2120	44555	0.50974	4312	90601	0.54353
22	1196	26491	0.46293	3364	74275	0.50980	7074	156027	0.54354
23	1824	41953	0.46280	5368	123465	0.50973	11682	268687	0.54353
24	2768	66703	0.46283	8551	205743	0.50977	19248	462703	0.54354
25	4240	106011	0.46285	13698	342461	0.50976	31872	796811	0.54353
26	6454	168223	0.46281	21899	570131	0.50975	52729	1372127	0.54353
27	9906	267535	0.46285	35154	949255	0.50976	87512	2362957	0.54353
≤ 27	28732	720485	0.46285	93809	2374821	0.50976	221219	5632249	0.54353

5 Conclusions

An efficient systematic method to locate and prove the existence of periodic windows was introduced. The method is based on the symbolic dynamics based approach to locate unstable periodic orbits (UPOs) and the continuation method to find periodic windows. Symbolic dynamics representation of trajectories is used to find initial guesses for positions of periodic orbits. It is also used to exclude certain symbol sequences to speed up the search process in finding periodic orbits and to select symbol sequences which may lead to periodic windows in the region of interest. The classical method of finding periodic windows which is based on the construction of bifurcation diagrams is not capable of finding narrow periodic windows due to the necessity of very fine sampling of the parameter space and long convergence times to observe periodic attractors existing for narrow periodic windows. The proposed method was applied to study the existence of periodic windows for the Rössler system in a region of the parameter space close to the classical parameter values. Several thousands of periodic windows have been identified, their existence was proved using rigorous computational methods and lower bounds on the measure of the set of regular parameters was computed. Periodic attractors existing for parameter values very close to the classical case $(a, b) = (5.7, 0.2)$ were found. More precisely, it was proved that there exist periodic attractors for $(a, b) = (5.699999143892, 0.2)$ and $(a, b) = (5.7, 0.2000000949446)$.

References

- [1] R. May, "Simple mathematical models with very complicated dynamics," *Nature*, vol. 261, pp. 459–467, 1976.
- [2] M. Hénon, "A two dimensional map with a strange attractor," *Commun. Math. Phys.*, vol. 50, pp. 69–77, 1976.
- [3] R. Gilmore and M. Lefranc, *The Topology of Chaos*. Wiley, 2011.

Table 4: Period windows existing for $(a, b) \in \{5.7\} \times [0.175, 0.215]$, W_p is the number of period- p windows found, w_p is the total width of period- p windows, $W_{p,PR}$ and $w_{p,PR}$ are the number and the total width of primary period- p windows found, $W_{p,PD}$ is the number of period-doubling windows found.

p	W_p	w_p	$w_{p,\max}$	$W_{p,PR}$	$w_{p,PR}$	$w_{p,PR,\max}$	$W_{p,PD}$
3	1	$5.894 \cdot 10^{-3}$	$5.894 \cdot 10^{-3}$	1	$5.894 \cdot 10^{-3}$	$5.894 \cdot 10^{-3}$	0
6	1	$3.034 \cdot 10^{-3}$	$3.034 \cdot 10^{-3}$	0	0	0	1
7	1	$5.221 \cdot 10^{-5}$	$5.221 \cdot 10^{-5}$	1	$5.221 \cdot 10^{-5}$	$5.221 \cdot 10^{-5}$	0
8	3	$1.035 \cdot 10^{-4}$	$5.522 \cdot 10^{-5}$	3	$1.035 \cdot 10^{-4}$	$5.522 \cdot 10^{-5}$	0
9	3	$1.004 \cdot 10^{-4}$	$9.465 \cdot 10^{-5}$	2	$5.776 \cdot 10^{-6}$	$3.898 \cdot 10^{-6}$	0
10	7	$2.089 \cdot 10^{-5}$	$8.963 \cdot 10^{-6}$	7	$2.089 \cdot 10^{-5}$	$8.963 \cdot 10^{-6}$	0
11	10	$1.975 \cdot 10^{-5}$	$8.330 \cdot 10^{-6}$	10	$1.975 \cdot 10^{-5}$	$8.330 \cdot 10^{-6}$	0
12	18	$7.188 \cdot 10^{-4}$	$7.100 \cdot 10^{-4}$	16	$4.938 \cdot 10^{-6}$	$1.643 \cdot 10^{-6}$	1
13	29	$9.813 \cdot 10^{-6}$	$4.070 \cdot 10^{-6}$	29	$9.813 \cdot 10^{-6}$	$4.070 \cdot 10^{-6}$	0
14	49	$3.134 \cdot 10^{-5}$	$2.621 \cdot 10^{-5}$	48	$5.126 \cdot 10^{-6}$	$1.770 \cdot 10^{-6}$	1
15	81	$2.856 \cdot 10^{-5}$	$2.284 \cdot 10^{-5}$	78	$1.729 \cdot 10^{-6}$	$1.794 \cdot 10^{-7}$	0
16	135	$5.491 \cdot 10^{-5}$	$2.807 \cdot 10^{-5}$	132	$2.607 \cdot 10^{-6}$	$8.333 \cdot 10^{-7}$	3
17	227	$2.066 \cdot 10^{-6}$	$7.093 \cdot 10^{-7}$	227	$2.066 \cdot 10^{-6}$	$7.093 \cdot 10^{-7}$	0
18	376	$8.022 \cdot 10^{-5}$	$4.434 \cdot 10^{-5}$	369	$1.404 \cdot 10^{-6}$	$8.302 \cdot 10^{-7}$	3
19	632	$9.973 \cdot 10^{-7}$	$3.055 \cdot 10^{-7}$	632	$9.973 \cdot 10^{-7}$	$3.055 \cdot 10^{-7}$	0
20	1052	$1.118 \cdot 10^{-5}$	$4.470 \cdot 10^{-6}$	1045	$7.480 \cdot 10^{-7}$	$3.469 \cdot 10^{-7}$	7
21	1762	$8.936 \cdot 10^{-6}$	$4.182 \cdot 10^{-6}$	1752	$4.476 \cdot 10^{-7}$	$2.001 \cdot 10^{-7}$	0
22	2944	$1.031 \cdot 10^{-5}$	$4.148 \cdot 10^{-6}$	2934	$4.327 \cdot 10^{-7}$	$1.596 \cdot 10^{-7}$	10
23	4929	$6.372 \cdot 10^{-7}$	$2.808 \cdot 10^{-7}$	4929	$6.372 \cdot 10^{-7}$	$2.808 \cdot 10^{-7}$	0
24	8249	$1.669 \cdot 10^{-4}$	$1.561 \cdot 10^{-4}$	8214	$1.353 \cdot 10^{-7}$	$1.596 \cdot 10^{-8}$	18
25	13816	$1.905 \cdot 10^{-7}$	$9.357 \cdot 10^{-8}$	13816	$1.905 \cdot 10^{-7}$	$9.357 \cdot 10^{-8}$	0
26	23152	$5.099 \cdot 10^{-6}$	$2.047 \cdot 10^{-6}$	23123	$1.819 \cdot 10^{-7}$	$1.196 \cdot 10^{-7}$	29
27	38803	$4.170 \cdot 10^{-6}$	$1.738 \cdot 10^{-6}$	38773	$6.165 \cdot 10^{-8}$	$9.529 \cdot 10^{-9}$	0
≤ 27	96280	$1.036 \cdot 10^{-2}$	$5.894 \cdot 10^{-3}$	96141	$6.127 \cdot 10^{-3}$	$5.894 \cdot 10^{-3}$	73
28–160	3567	$1.674 \cdot 10^{-4}$	$3.359 \cdot 10^{-5}$	0	0	0	408
all	99847	$1.053 \cdot 10^{-2}$	$5.894 \cdot 10^{-3}$	96141	$6.127 \cdot 10^{-3}$	$5.894 \cdot 10^{-3}$	481

- [4] W. Tucker and D. Wilczak, “A rigorous lower bound for the stability regions of the quadratic map,” *Physica D*, vol. 238, no. 18, pp. 1923–1936, 2009.
- [5] Z. Galias and W. Tucker, “Is the Hénon attractor chaotic?” *Chaos: Interdiscipl. J. Nonlinear Sci.*, vol. 25, no. 3, p. 033102 (12 pages), 2015.
- [6] O. Roessler, “An equation for continuous chaos,” *Physics Letters*, vol. 35A, pp. 397–398, 1976.
- [7] C. Letellier, P. Dutertre, and B. Maheu, “Unstable periodic orbits and templates of the Rössler system: Toward a systematic topological characterization,” *Chaos: An Interdisciplinary Journal of Nonlinear Science*, vol. 5, no. 1, pp. 271–282, 1995.
- [8] P. Zgliczyński, “Computer assisted proof of chaos in the Rössler equations and in the Hénon map,” *Nonlinearity*, vol. 10, no. 1, pp. 243–252, 1997.
- [9] Z. Galias, “Counting low-period cycles for flows,” *Int. J. Bifurcation Chaos*, vol. 16, no. 10, pp. 2873–2886, 2006.
- [10] D. Wilczak and P. Zgliczyński, “Period doubling in the Rössler system—a computer assisted proof,” *Foundations of Computational Mathematics*, vol. 9, no. 5, pp. 611–649, 2009.
- [11] R. Barrio, F. Blesa, and S. Serrano, “Qualitative analysis of the Rössler equations: Bifurcations of limit cycles and chaotic attractors,” *Physica D: Nonlinear Phenomena*, vol. 238, no. 13, pp. 1087–1100, 2009.
- [12] Y. Saiki and M. Yamada, “Time-averaged properties of unstable periodic orbits and chaotic orbits in ordinary differential equation systems,” *Phys. Rev. E*, vol. 79, p. 015201, Jan 2009.
- [13] S. Malykh, Y. Bakhanova, A. Kazakov, K. Pusuluri, and A. Shilnikov, “Homoclinic chaos in the Rössler model,” *Chaos: An Interdisciplinary Journal of Nonlinear Science*, vol. 30, no. 11, p. 113126, 2020.

- [14] D. Wilczak, S. Serrano, and R. Barrio, “Coexistence and dynamical connections between hyperchaos and chaos in the 4d Rössler system: A computer-assisted proof,” *SIAM Journal on Applied Dynamical Systems*, vol. 15, pp. 356–390, Jan 2016.
- [15] M. R. Candido, D. D. Novaes, and C. Valls, “Periodic solutions and invariant torus in the Rössler system,” *Nonlinearity*, vol. 33, no. 9, p. 4512, Jul 2020.
- [16] A. Gierzkiewicz and P. Zgliczyński, “From the Sharkovskii theorem to periodic orbits for the Rössler system,” *Journal of Differential Equations*, vol. 314, pp. 733–751, 2022.
- [17] “CAPD library,” <http://capd.ii.uj.edu.pl/>, 2024.
- [18] T. Kapela, M. Mrozek, D. Wilczak, and P. Zgliczyński, “CAPD::DynSys: a flexible C++ toolbox for rigorous numerical analysis of dynamical systems,” *Communications in Nonlinear Science and Numerical Simulation*, vol. 101, p. 105578, 2020.
- [19] “GNU MPFR library,” <http://www.mpfr.org>, 2024.
- [20] Z. Galias, “Continuation-based method to find periodic windows in bifurcation diagrams with applications to the Chua’s circuit with a cubic nonlinearity,” *IEEE Trans. Circuits Syst. I, Reg. Papers*, vol. 68, no. 9, pp. 3784–3793, 2021.
- [21] —, “A fast method to find periodic orbits in chaotic attractors with applications to the Rössler system,” *IEEE Trans. Circuits Syst. II, Exp. Briefs*, vol. 70, no. 9, pp. 3659–3663, 2023.
- [22] A. Neumaier, *Interval Methods for Systems of Equations*. Cambridge, UK: Cambridge University Press, 1990.
- [23] N. Metropolis, M. Stein, and P. Stein, “On finite limit sets for transformations on the unit interval,” *Journal of Combinatorial Theory, Series A*, vol. 15, no. 1, pp. 25–44, 1973.
- [24] Z. Wan-Zhen, H. Bai-Lin, W. Guang-Rui, and C. Shi-Gang, “Scaling property of period-n-tupling sequences in one-dimensional mappings,” *Communications in Theoretical Physics*, vol. 3, no. 3, p. 283, 1984.
- [25] Z. Galias, “Systematic search for wide periodic windows and bounds for the set of regular parameters for the quadratic map,” *Chaos: Interdiscipl. J. Nonlinear Sci.*, vol. 27, no. 5, p. 053106, 2017.